Silver Nanoparticles Impregnated Zeolites Derived from Coal Fly Ash: Effect of the Silver Loading on Adsorption of Mercury (II) †

Zhandos Tauanov, Dhawal Shah and Vassilis Inglezakis *

School of Engineering, Chemical Engineering Department, Environmental Science & Technology Group (ESTg), Nazarbayev University, Astana 010000, Kazakhstan; zhtauanov@nu.edu.kz (Z.T.); dhawal.shah@nu.edu.kz (D.S.)

* Correspondence: vasileios.inglezakis@nu.edu.kz; Tel.: +1-771-7270-6534

† Presented at the 3rd EWaS International Conference on "Insights on the Water-Energy-Food Nexus", Lefkada Island, Greece, 27–30 June 2018.

Abstract: Removal of mercury (II) from aqueous phase is of utmost importance, as it is highly toxic and hazardous to the environment and human health. A promising method for the removal of mercury (II) ions from aqueous solutions is by using adsorbents derived from coal fly ash (CFA), such as synthetic zeolites. In this work we present the hydrothermal production of synthetic zeolites from CFA followed by a modification for impregnation of silver nanoparticles, in solid concentrations from 0.15 to 4.71 wt.%. All produced zeolites and parent materials are characterized by XRD, XRF, BET and PSA to obtain morphological and microstructural data. Moreover, mercury (II) ions removal from aqueous solutions with initial concentration of 10 ppm is studied. According to results, zeolites and Ag-nanocomposites demonstrate much higher removal than parent CFA (up to 98%). In addition to this, we could observe a distinct adsorption behavior depending on the loading of Ag NPs in nanocomposites. A possible removal mechanism for both zeolites and Ag-nanocomposites is discussed.

Keywords: coal fly ash; mercury removal; nanocomposites; silver nanoparticles; synthetic zeolite

1. Introduction

Coal fly ash (CFA) is a value-added by-product produced from combustion of coal in power stations all over the world. The amount of annually discharged CFA is enormous and thus it requires further investigation on the reprocessing, as it causes serious environmental and health issues [1,2]. Kazakhstan, for example, produces almost 19 million tons of CFA per year and has already accumulated 300 million tons of by-products in ash-disposal area [3]. As the demand for energy grows tremendously, and taking into account a heavy dependence of the electricity production of Kazakhstan on coal industry it is very important for the country to dispose of CFA in a safely manner that is not harmful to the environment and health. According to statistics just under 10% of all fly ash is utilized in the country, which is far below the indexes in other countries as the US (nearly 50%), EU states (over 90%), China (67%) and India (60%) [4].

One of the efficient ways of utilizing CFA is converting into various types of zeolites [5,6], and produced materials could be applied for adsorption of heavy metals [7,8]. An issue that is questioned by many researchers around the world is the contamination of water resources with heavy metals, particularly with mercury (II) and its species. Mercury, due to its volatility, persistence and bioaccumulation properties, is considered as one of the most toxic elements that severely affect human beings and environment [9]. A prolonged exposure to mercury and its species

are considered to harm a human brain, heart, kidneys, lungs and the whole immune system [10], [11].

More studies that are recent include synthetic and natural zeolites and their composites that contain metal(s) or metal oxide(s) nanoparticles (NPs) or combination of them, which in turn further expands the application fields. Among all mentioned metal and metal-oxide containing composites, a particular interest lies on silver and silver oxide NPs containing zeolite nanocomposites, since they possess unique property to form amalgams with mercury [12]. According to current regulations of the US Environmental Protection Agency (EPA) the maximum contaminant level (MCL) of mercury concentration is 0.2 ppb (or 0.2 um/L) [13]. In this work we present a conversion of locally available CFA into synthetic zeolite by subsequent impregnation of silver nanoparticles and producing novel nanocomposite. The produced nanocomposites and their parent materials are tested for mercury (II) remediation from aqueous phase and the possible adsorption mechanisms is discussed.

2. Materials and Methods

2.1. Materials

All reagents in this work were of analytical grade and used as received without prior purification. A representative col fly ash (CFA) sample, namely Karazhyra CFA was collected from the electrostatic precipitators of Oskemen city power station (East Kazakhstan, 252 MW). Particularly, silver nitrate ($AgNO_3$, 99.9%) and sodium hydroxide pearls (NaOH, 99.5%) were supplied by Sigma-Aldrich, sodium borohydride ($NaBH_4$, 99.9%) and mercury (II) chloride ($HgCl_2$, 99.9%) were purchased from Fischer-Scientific. Concentrated and dilute solutions of nitric acid and sodium hydroxide were used to adjust the pH to 2.0 that is suitable for batch adsorption experiments.

In order to simplify the notation of raw and derived materials, following code names were given for CFA, their derived synthetic zeolites and nanocomposite materials: Karazhyra CFA was denoted as K-CFA, synthetic zeolite derived from K-CFA denoted as K-ZFA and the nanocomposite materials with silver nanoparticles (Ag NPs) were labeled as X%-Ag-K-ZFA, where X is the loading of Ag NPs in nanocomposite structure that varies: 0.15, 0.34, 0.92 and 4.71 wt.%. In addition to this, reduced K-ZFA samples was used and denoted as R-K-ZFA.

2.2. Synthesis of Zeolites and Nanocomposites

To produce synthetic zeolite K-ZFA a conventional hydrothermal alkaline treatment was applied. Sodium hydroxide was selected as an activation agent based on previous experience in synthesis of zeolite [7,14]. The detailed synthesis procedure is explained in our previous work elsewhere [15].

The produced K-ZFA was loaded with various amounts of silver nanoparticles (Ag NPs) in order to produce and examine the novel nanocomposite materials for mercury removal. The Ag NPs impregnation into the structure of zeolites consists of two main steps: ion exchange and reduction. Initially, K-ZFA was fully dried at 300 °C for 3 h in order to remove any remaining water molecules or organic matter. Then, a slightly modified ion-exchange reaction [16,17] was conducted by adding 10 mmol/L solution of $AgNO_3$ with various volumes depending on the target loading of Ag NPs (2–20 mL per 1 g of zeolite) and left to cure for 12 h. Each reaction container was covered with aluminum foil in order to prevent oxidation of silver ions. After that the obtained soaked zeolite slurry was dried at 130 °C for 3 h. The same soaking procedure was repeated to produce silver ion-exchanged zeolites (Ag^+-ZFA). The obtained Ag^+-ZFA was then subjected to calcination for 3 h at 500 °C, followed by 4 h silver ions reduction using $NaBH_4$, thus producing nanocomposites with various Ag NPs loadings (X%-Ag-K-ZFA). Similar procedure was carried out for an R-K-ZFA sample with adding deionized water instead of silver nitrate solution. This was done in order to investigate the effect of reduction onto zeolite structure and adsorption capacity.

2.3. Characterization of Materials

X-ray Diffraction (XRD) instrument (Rigaku, Tokyo, Japan) was used to obtain information on mineralogical phases present in all samples. The XRD pattern was recorded on a SmartLab X-ray diffraction instrument (Cu, K-β filter, 40 kV and 30 mA) with a diffraction angle of 2θ and a scanning range of 5–100°. The phase identification was conducted by applying an auto-search tool of powder diffraction file library.

X-ray Fluorescence (XRF, PANalytical Axios, Cambridge, UK) instrument was applied to get the elemental composition of CFAs and ZFAs. The CFA sample was analyzed as received without prior purification and sieving; whereas all produced ZFAs were washed and dried beforehand. The ratio of sample with binder was set at 10 g to 3 g (total mass of 13 g) with a diameter of pellet at 5 cm and thickness of pellet at 0.5 cm. The analyses were duplicated and conducted under inert atmosphere. A nitrogen Porosimeter (Autosorb-1, Quantachrome, Hook, UK) was applied to obtain data on BET surface area, average pore size and total volume. The samples of fly ash were first degassed for 3 h prior to analysis at stepwise heating from 50 °C to 110 °C. A 9 mm glass cell without rod was used for all porosimetric studies. Particle size analyzer (Mastersizer 3000, Malvern, Cambridge, UK) was used to measure the particle size distribution. The samples were analyzed using hydro-mode at room temperature, where deionized water used as a dispersion solution.

2.4. Batch Adsorption Kinetics

All produced materials and their respective parent CFAs were tested for their batch adsorption capacity in simulated water solutions of mercury (II) with initial concentration of 10 ppm. Mercury analyzer (RA-915 M, Lumex, St. Petersburg, Russia) was used to quantify the amount of mercury (II) adsorbed. All adsorption experiments were carried out in duplication without stirring and at room temperature. The detailed description of mercury analysis and experimental conditions are written in our previous work elsewhere [15].

## 3. Results and Discussion

3.1. Characterization of Materials

The phase composition results of CFA, ZFA and Ag NPs containing nanocomposites are shown in Figure 1. As it is seen from the XRD spectra the main phases of CFA are mullite, quartz and magnetite. The zeolitization of raw CFA produced a synthetic zeolite analcime with conversion value of up to 65%. The Ag NPs impregnated nanocomposites produced from K-ZFA show the specific major peaks of Ag NPs at 38.16, 44.32 and 64.56 that confirms the formation of composite. It is more detectable in 0.92 wt.%-Ag-K-ZFA and 4.71 wt.%-Ag-K-ZFA nanocomposites samples than in lower Ag NPs containing materials 0.15 wt.%-Ag-K-ZFA and 0.34 wt.%-Ag-K-ZFA.

The BET analysis of materials show that on average the lowest surface area is observed for K-CFA (18 m²/g), whereas the highest surface is measured for nanocomposites (Table 1). The representative nanocomposite 4.71 wt.%-Ag-K-ZFA (105.3 m²/g) revealed almost 6 fold BET surface area than parent K-CFA. These leads to the conclusion that the microstructure and porosity drastically improves from parent CFA, ZFA to nanocomposite. These physical and chemical property changes should positively affect the adsorption capacity of the material, as it creates more active sites for mercury to be adsorbed.

Table 1. BET surface areas of materials.

Material Type	BET Surface Area, m²/g
CFA	18.08 ± 14.92
ZFA	55.80 ± 12.20
R-ZFA	38.00 ± 8.00
4.71 wt.%-Ag-ZFA	105.30 ± 12.30
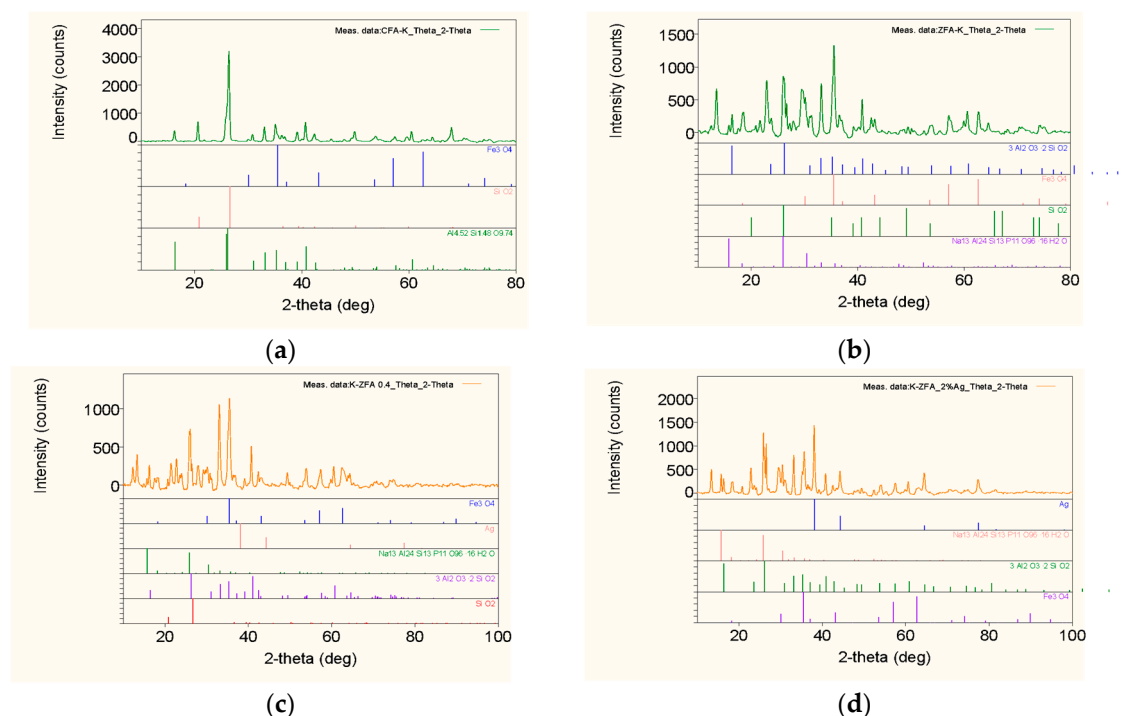
Figure 1. XRD spectra of raw and produced materials: (**a**) K-CFA; (**b**) K-ZFA; (**c**) 0.34 wt.%-Ag-K-ZFA; (**d**) 4.71 wt.%-Ag-K-ZFA.

Table 2 demonstrates the results of chemical composition of parent CFA and synthesized materials. It is clear from the results obtained that the main compounds with higher fractions are Na_2O, Al_2O_3, SiO_2 CaO, Fe_2O_3. It should be noted that local K-CFA is rich for magnetite, which is confirmed by XRD and XRF analysis and comparatively higher than in other CFA samples around the world [5,18]. The Si/Al ratio of K-ZFA is 0.93, these results are comparable with data obtained elsewhere [5,6,19]. The nanocomposites, on the other hand, show a composition of Ag_2O, which is the oxidized form of Ag NPs, which confirms the formation of nanocomposite with various Ag NPs loading.

Another important characterization results is the particle size analysis. According to reults shown in Table 3, the lowest particle size was observed for K-R-ZFA with 50% of particles at 8.04 μm, followed by nanocomposites (12.45–13.20 μm, K-ZFA (25.54 μm) and CFA (57.43 μm). These obtained data will assist in explaining the dominating mechanism and kinetics of adsorption in materials.
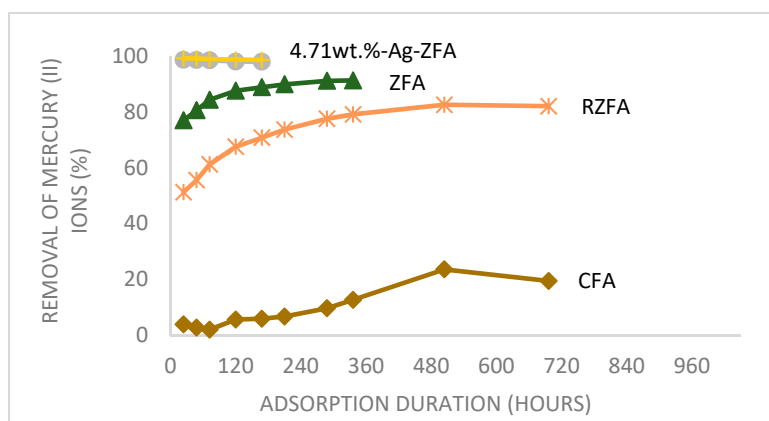
3.2. Batch Adsorption Kinetics

According to the adsorption results Ag NPs containing composite 4.71 wt.%-Ag-ZFA showed 98.73% removal of Hg^{2+} in just 24 h, which is approximately 10% higher than in K-ZFA. The lowest adsorption value was demonstrated by K-CFA (9.7%) that could be explained by a lower BET surface area demostrated on surface area analysis. It should be noted that K-ZFA, K-R-ZFA and K-CFA reached equilibriums after 14 days, 21 days and 29 days, accordingly (Figure 2), which could be related to both particle sizes and different adsorption mechanisms than in nanocomposites.

Table 2. Chemical composition of materials.

Compounds	K-CFA	K-ZFA	0.2 wt.%-Ag-K-ZFA	0.4 wt.%-Ag-K-ZFA	1.0 wt.%-Ag-K-ZFA	2.0 wt.%-Ag-K-ZFA
Na_2O	0.678	4.447	4.369	4.272	3.557	3.405
MgO	0.716	0.708	0.758	0.677	0.651	0.646
Al_2O_3	25.761	30.888	29.984	29.637	29.201	28.245
SiO_2	49.802	32.488	31.596	31.357	31.237	30.959
SO_3	0.237	0.086	0.076	0.080	0.060	0.047
K_2O	1.324	0.150	0.142	0.172	0.141	0.119
CaO	2.798	2.390	2.332	2.274	2.162	2.089
TiO_2	1.636	1.258	1.156	1.111	1.159	1.142
Cr_2O_3	0.033	3.104	3.302	3.174	2.890	3.359
MnO	0.216	0.411	0.482	0.491	0.466	0.463
Fe_2O_3	16.076	23.066	24.595	25.340	26.494	22.389
Co_3O_4	0.028	0.061	0.068	0.068	0.060	0.060
NiO	0.032	0.432	0.455	0.457	0.435	0.383
CuO	0.042	0.028	0.034	0.035	0.025	0.025
ZnO	0.052	0.040	0.038	0.035	0.040	0.033
SrO	0.195	0.206	0.197	0.197	0.177	0.167
Y_2O_3	0.012	0.013	0.012	0.012	0.012	0.018
ZrO_2	0.06	0.074	0.079	0.040	0.072	0.070
Ag_2O	0	0	0.161	0.361	0.989	5.056
BaO	0.143	0.119	0.109	0.118	0.118	0.109
CeO_2	0.126	0	0.055	0.093	0.054	0.068

Table 3. PSD analysis of materials.

PSD	K-CFA	K-ZFA	4.71 wt%-Ag-ZFA	0.92 wt.%-Ag-ZFA	K-R-ZFA
$Dv(10)$, μm	22.06 ± 2.40	5.69 ± 0.31	2.44 ± 0.01	2.50 ± 0.01	1.75 ± 0.05
$Dv(50)$, μm	57.43 ± 0.03	25.54 ± 0.83	13.20 ± 0.02	12.45 ± 0.05	4 ± 0.03
$Dv(90)$, μm	161.33 ± 5.66	65.80 ± 0.80	55.65 ± 0.05	61.1 ± 1.60	41.53 ± 4.36

Figure 2. Adsorption kinetics of Hg^{2+} from aqueous media.

As it is seen from Figure 2, the adsorption kinetics of zeolite and nanocomposite differ. We hypothesize that it might be due to particle size and different adsorption mechanisms in these materials. As we know from characterization results, on average the PSD of nanocomposite is smaller than of zeolites, which could explain this behavior in adsorption kinetics. However, the PSD analysis of K-R-ZFA is even finer than particle sizes of nanocomposite, which lays the foundation for different adsorption mechanism in the latter.

In order to explain the difference in both adsorption kinetics and capacity, another synergetic and possibly major explanation is needed. It could be a diverse mechanism of adsorption in nanocomposite that is resulted from redox reaction of $Ag°/Ag^+$ (+0.80 V) and $Hg^{2+}/Hg°$ (+0.85 V) [20], which occurs due to close redox potentials of two metals. A distinct decrease of Ag NPs major peaks and formation of AgCl on XRD of 4.71 wt.%-Ag-ZFA after adsorption with 10 ppm $HgCl_2$ solution could be observed in Figure 3. The obtained results led to the assumption that the one of the adsorption mechanisms of nanocomposite could be the formation of an amalgam between two metals Ag_xHg_y and/or precipitation of $Hg°$ on the surface and microstructure. Thus, it could be proposed that the novel nanocomposite has advantages over the existing CFA-derived materials

[21,22], since 4.71 wt.%-Ag-ZFA almost fully and fastly remove mercury ions from water phase and allows to overcome a redox reaction that forms a very stable amalgam/complex, which in turn reduces the leaching of adsorbed mercury to avoid further environmental issues.

Figure 4 shows the kinetcis of the Hg^{2+} adsorption of nanocomposites with various loadings. According to these results the loading of Ag NPs in the structure of composite is directly related to the adsorption capacity and kinetics. For example, 0.15 wt.%-Ag-ZFA removed 79.7% of Hg^{2+} in 9 days, whereas 0.92 wt.% Ag-ZFA could remove up to 96.36% in just 2 days. It should be noted that average particles size of all nanocomposites is the same, thus the kinetics in this material is related to loading of nanoparticles.
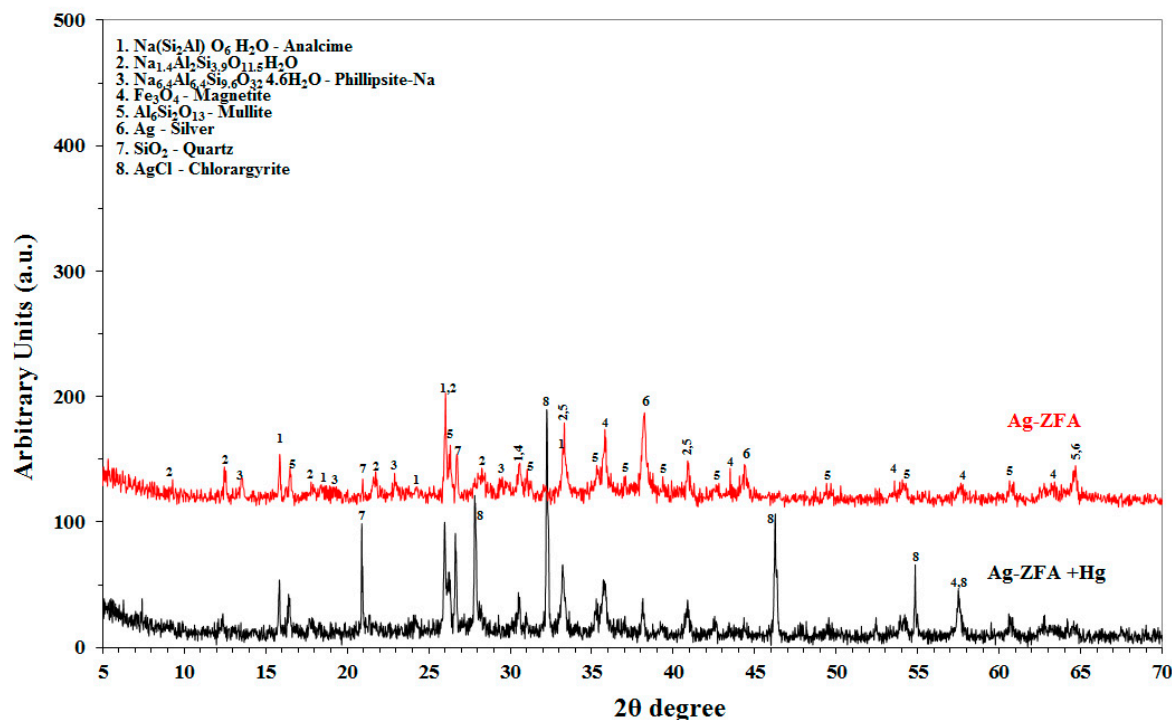

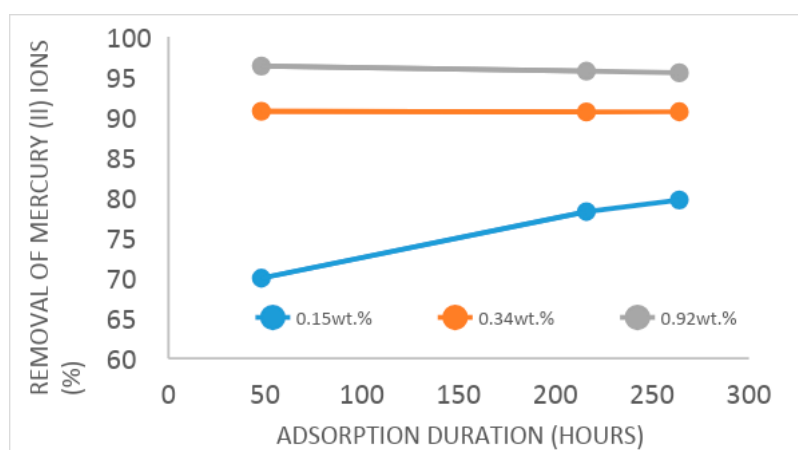**Figure 3.** XRD spectra of Ag-ZFA and 4.71 wt.% Ag-ZFA with Hg (II).

Figure 4. A comparative Hg^{2+} adsorption capacity of nanocomposites.

4. Conclusions

The synthetic zeolite and novel nanocomposite containing various loadings of Ag NPs in microstructure were successfully produced from parent K-CFA sample. All produced and parent materials were examined for mercury (II) removal potential using simulated solutions under acidic

conditions. The results revealed that all nanocomposites were effective in removing Hg^{2+} from aqueous media in contrast with parent K-CFA and K-R-ZFA. The K-ZFA showed a comparable adsorption capacity as nanocomposite 0.34 wt.%-Ag-ZFA, whereas the nanocomposites with higher loadings of Ag NPs revealed improved adsorption (96.36% and 98.76%). It was found out that nanocomposites show a direct correlation with Ag NPs loading in terms of adsorption capacity and follow this order: 0.15 wt.%-Ag-ZFA < 0.34 wt.%-Ag-ZFA < 0.92 wt.%-Ag-ZFA < 4.71 wt.%-Ag-ZFA. The tentative conclusions on the mechanism of removal is that it might be a combination of physical adsorption, precipitation of mercury as $Hg°$ and amalgamation of two metals as Ag_xHg_y.

Author Contributions: Z.T. designed and performed the experiments, wrote the paper; D.S. and G.I. analyzed the data; V.I. reviewed the paper and managed the whole work.

Conflicts of Interest: The authors declare no conflict of interest.

References

1. Bukhari, S.S.; Behin, J.; Kazemian, H.; Rohani, S. Conversion of coal fly ash to zeolite utilizing microwave and ultrasound energies: A review. *Fuel* **2015**, *140*, 250–266.
2. Blissett, R.S.; Rowson, N.A. A review of the multi-component utilisation of coal fly ash. *Fuel* **2012**, *97*, 1–23.
3. Tauanov, Z.; Abylgazina, L.; Spitas, C.; Itskos, G.; Inglezakis, V. Mineralogical, Microstructural and Thermal Characterization of Coal Fly Ash Produced from Kazakhstani Power Plants. *IOP Conf. Ser. Mater. Sci. Eng.* **2017**, *230*, 012046.
4. Yao, Z.T.; Ji, X.S.; Sarker, P.K.; Tang, J.H.; Ge, L.Q.; Xia, M.S.; Xi, Y.Q. A comprehensive review on the applications of coal fly ash. *Earth Sci. Rev.* **2015**, *141*, 105–121.
5. Chansiriwat, W.; Tanangteerapong, D.; Wantala, K. Synthesis of zeolite from coal fly ash by hydrothermal method without adding alumina and silica sources: Effect of aging temperature and time. *Sains Malays.* **2016**, *45*, 1723–1731.
6. Xie, J.; Wang, Z.; Wu, D.; Kong, H. Synthesis and properties of zeolite/hydrated iron oxide composite from coal fly ash as efficient adsorbent to simultaneously retain cationic and anionic pollutants from water. *Fuel* **2014**, *116*, 71–76.
7. Koukouzas, N.; Vasilatos, C.; Itskos, G.; Mitsis, I.; Moutsatsou, A. Removal of heavy metals from wastewater using CFB-coal fly ash zeolitic materials. *J. Hazard. Mater.* **2010**, *173*, 581–588.
8. Visa, M.; Chelaru, A.M. Hydrothermally modified fly ash for heavy metals and dyes removal in advanced wastewater treatment. *Appl. Surf. Sci.* **2014**, *303*, 14–22.
9. Yu, J.G.; Yue, B.Y.; Wu, X.W.; Liu, Q.; Jiao, F.P.; Jiang, X.Y.; Chen, X.Q. Removal of mercury by adsorption: A review. *Environ. Sci. Pollut. Res.* **2016**, *23*, 5056–5076.
10. Hsiao, H.W.; Ullrich, S.M.; Tanton, T.W. Burdens of mercury in residents of Temirtau, Kazakhstan: I: Hair mercury concentrations and factors of elevated hair mercury levels. *Sci. Total Environ.* **2011**, *409*, 2272–2280.
11. Hsiao, H.W.; Ullrich, S.M.; Tanton, T.W. Burdens of mercury in residents of Temirtau, Kazakhstan: II: Verification of methodologies for estimating human exposure to high levels of Hg pollution in the environment. *Sci. Total Environ.* **2010**, *408*, 4033–4044.
12. Wdowin, M.; Wiatros-Motyka, M.M.; Panek, R.; Stevens, L.A.; Franus, W.; Snape, C.E. Experimental study of mercury removal from exhaust gases. *Fuel* **2014**, *128*, 451–457.
13. AMAP/UNEP. *Technical Background Report for the Global Mercury Assessment*; Arctic Monitoringand Assessment Programme: Oslo, Norway, 2013. Available online: www.amap.no/documents/doc/technical-background-report-for-the-global-mercury-assessment-2013/848 (accessed on 14 May 2018).
14. Itskos, G.; Koutsianos, A.; Koukouzas, N.; Vasilatos, C. Zeolite development from fly ash and utilization in lignite mine-water treatment. *Int. J. Miner. Process.* **2015**, *139*, 43–50.

15. Tauanov, Z.; Shah, D.; Itskos, G.; Inglezakis, V. Optimized Production of Coal Fly Ash Derived Synthetic Zeolites for Mercury Removal from Wastewater. *IOP Conf. Ser. Mater. Sci. Eng.* **2017**, *230*, 012044.

16. Golubeva, O.Y.; Ternovaya, N.Y.; Maltseva, N.V.; Meyerstein, D. Catalytic hydrogen oxidation using zeolite RHO modified by silver nanoparticles. *Glass Phys. Chem.* **2012**, *38*, 455–459.

17. Golubeva, O.Y.; Ulyanova, N.Y.; Kurilenko, L.N. Synthesis and study of catalytic activity of zeolite Rho with varying content of silver nanoparticles. *Glass Phys. Chem.* **2013**, *39*, 649–653.

18. Hu, T.; Gao, W.; Liu, X.; Zhang, Y.; Meng, C. Synthesis of zeolites Na-A and Na-X from tablet compressed and calcined coal fly ash. *R. Soc. Open Sci.* **2017**, *4*, 170921.

19. Jha, V.K.; Matsuda, M.; Miyake, M. Sorption properties of the activated carbon-zeolite composite prepared from coal fly ash for Ni^{2+}, Cu^{2+}, Cd^{2+} and Pb^{2+}. *J. Hazard. Mater.* **2008**, *160*, 148–153.

20. Henglein, A.; Brancewicz, C. Absorption spectra and reactions of colloidal bimetallic nanoparticles containing mercury. *Chem. Mater.* **1997**, *4756*, 2164–2167.

21. Attari, M.; Bukhari, S.S.; Kazemian, H.; Rohani, S. A low-cost adsorbent from coal fly ash for mercury removal from industrial wastewater. *J. Environ. Chem. Eng.* **2017**, *5*, 391–399.

22. Czarna, D.; Baran, P.; Kunecki, P.; Panek, R.; Zmuda, R.; Wdowin, M. Synthetic zeolites as potential sorbents of mercury from wastewater occurring during wet FGD processes of flue gas. *J. Clean. Prod.* **2016**, *172*, 2636–2645.